Photochemical & Photobiological Sciences

Accepted Manuscript

This is an *Accepted Manuscript*, which has been through the Royal Society of Chemistry peer review process and has been accepted for publication.

Accepted Manuscripts are published online shortly after acceptance, before technical editing, formatting and proof reading. Using this free service, authors can make their results available to the community, in citable form, before we publish the edited article. We will replace this *Accepted Manuscript* with the edited and formatted *Advance Article* as soon as it is available.

You can find more information about *Accepted Manuscripts* in the Information for Authors.

Please note that technical editing may introduce minor changes to the text and/or graphics, which may alter content. The journal's standard Terms & Conditions and the Ethical guidelines still apply. In no event shall the Royal Society of Chemistry be held responsible for any errors or omissions in this *Accepted Manuscript* or any consequences arising from the use of any information it contains.

ROYAL SOCIETY OF CHEMISTRY

www.rsc.org/pps

Cite this: DOI: 10.1039/c0xx00000x

www.rsc.org/xxxxxx

ARTICLE TYPE

Extended Mechanistic Aspects on Photoinitiated Polymerization of 1,6-Hexanediol Diacrylate by Hexaarylbisimidazoles and Heterocyclic Mercapto Compounds

Stefan Berdzinski,[a] Nadine Strehmel,[b] Heike Lindauer,[c] Veronika Strehmel,[a*] and Bernd Strehmel[a*]

Received (in XXX, XXX) Xth XXXXXXXXX 20XX, Accepted Xth XXXXXXXXX 20XX
DOI: 10.1039/b000000x

Chlorine substituted hexaarylbisimidazole (*o*-Cl-HABI) efficiently initiates radical polymerization of multifunctional acrylic esters in the presence of a heterocyclic mercapto compound if the latter can form its tautomeric thione. Exposure of *o*-Cl-HABI results in lophyl radicals, which efficiently add to the thione in the first step while the second step releases a highly reactive thiyl radical from this intermediate. LC-MS and CID-MS measurements support this reaction scheme. Furthermore, photo-DSC experiments applying UV light between 320-380 nm showed that mercaptotriazole and phenylmercaptotriazole exhibited the best reactivity in the monomer 1,6-hexanediol diacrylate (HDDA) while alkyl substituted mercaptotriazoles showed less reactivity. Change of the triazole heterocycle by mercaptoimidazole resulted in a significant decrease of photoinitiation efficiency. This heterocycle does not form the corresponding thione in HDDA as shown by NMR measurements. Replacement of mercaptotriazole by an alkylthiol leads to a system showing the lowest photoinitiation efficiency in this series. Formation of thione structure in the case of heterocyclic mercapto compounds may cause the higher reactivity of the heterocyclic mercapto compounds with the lophyl radical in the monomer chosen.

1. Introduction

Substituted hexaarylbisimidazoles (HABI) have been known in photoinitiating systems for a long time[1-3]. These materials result in formation of lophyl radicals (L•) upon exposure by homolytic cleavage of the precursor **L-L** resulting in formation of purple colored relatively stable lophyl radicals (**L•**) as intermediates in ordinary solvents, eq. 1.

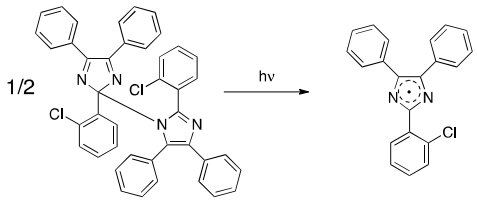

(1)

The efficiency of this reaction depends on the surrounding solvent, and how efficient **L•** can escape from the solvent cage[4-6]. Thus, the lifetime of the lophyl radical ranges between several minutes to hours in ordinary solvents down to milliseconds or microseconds choosing ionic liquids[4-6]. Nevertheless, the study of this photoreaction has got the attention of research with focus on both optical properties, such as photochromism[7-18], and magnetic properties, using ESR to explore the properties of the radicals generated and the cleavage mechanism. This can occur through a radical triplet-pair[19-25]. Furthermore, the efficient initiation of initiator systems containing HABI derivatives directed the use of such materials in holographic applications based on photopolymers[26-28].

Thus, hexaarylbisimidazoles have been widely applied in photoinitiating systems in radical polymerization, in which they either function as radical initiator in combination with a H-donating compound[1-3, 29] or in combination with a sensitizer, which donates an electron from its excited state to **L-L** resulting in formation of the lophyl radical (L•), lophin (**L**-H) and the oxidized form of the sensitizer[19, 21, 26-28, 30-37]. It has been also accepted that such sensitized systems require the addition of a H-donor; that is usually a heterocyclic mercapto compound. The generated reactive radical (L•) possesses the capability to abstract hydrogen from RS-H[3]. Further mechanistic discussions also include a mechanism based on energy transfer from a sensitizer to HABI. The triplet state of HABI lies relatively low (283 kJ/mol) and locates in the region of typical triplet sensitizers (isopropylthioxanthone: 272 kJ/mol, michlers ketone: 260 kJ/mol)[38]. Thus, triplet-triplet energy transfer would be possible in principle using an appropriate triplet sensitizer[38]. Furthermore, reference[21] critically compares both mechanisms relating either to energy transfer or electron transfer. The same authors investigated a sensitized HABI-system comprising three components; that was a sensitizer, a radical builder - the HABI -, and a radical initiator RS-H - the mercapto compound.

Furthermore, lophyl radicals extremely slow add to acrylic monomers. As mentioned above, initiation of photopolymerization generally requires the addition of a hydrogen donor (R'-H) resulting in formation of initiating radicals (R'•). Equation 2 shows the principal occurring steps, which has been accepted for several decades[1,2].

$$\mathbf{L}\bullet + RSH \longrightarrow ... \longrightarrow \mathbf{L\text{-}H} + RS\bullet \quad (2)$$

H-abstraction of the lophyl radical from RS-H was discussed as the major reaction[21, 26, 32-35, 39-48]. The RS• radical finally formed possesses a high reactivity to react with acrylic monomers resulting in initiation of photoinduced polymerization. Nowadays, there is no doubt that a hydrogen donor must be added to HABI upon exposure to obtain initiating radicals R• in high yield.

Direct exposure of **L-L** results in **L**•[1, 2] with a quantum yield of 1.96[1, 2,38] because absorption of one light quant by **L-L** results in formation of two **L**• radicals. The higher extinction coefficient in the UV compared to many commercial UV-initiators [49] could be seen as one advantage to apply such compounds as photoinitiator. Furthermore, photolytic formation of lophine (**L-H**) results in a significant hypsochromic shifted absorption in the presence of a hydrogen donating coinitiator (RSH). **L-H** shows no absorption at $\lambda > 350$ nm where HABI derivatives absorb. This makes HABI interesting for curing of coatings requiring a large depth profile because it can completely bleach above 350 nm.

Furthermore, different mercapto compounds were selected to initiate photopolymerization choosing various photosensitizers and **L-L**[32] to discuss the relation between reactivity and RS-H bond dissociation energy. All reactions discussed in reference[32] start from the excited state of the sensitizer. The thiyl radicals are generated by different reactions. These are direct reaction of the excited sensitizer with a mercapto compound on the one hand and reaction of the excited sensitizer with o-Cl-HABI resulting in lophyl radicals, which react with the mercapto compound in a secondary reaction on the other hand. Therefore, the thiyl radical concentration is influenced by various reactions, and decision about the contribution of the single reaction becomes difficult. In this contribution, we discuss the reaction of thiyl radical formation by direct excitation of **L-L** without any sensitizer. This may differ compared to a photoinitiating system comprising a photosensitizer, radical builder, and a radical initiator. Furthermore, we found, that the thiol-thione tautomerism has not received the necessary attention in previous studies, which should also influence the formation of initiating species. Therefore, we additionally studied the mechanism more in detail applying UPLC-ESI-QTOF-MS (ultra performance liquid chromatography electrospray ionization quadrupole time–of–flight mass spectrometry) to explore the structure of the compounds formed upon irradiation of the **L-L**/RSH System. We chose this hyphenation technique because UPLC provides the best opportunity to separate compounds from a complex mixture. The hybrid mass spectrometer ensures a high resolution in mass and the record of CID-MS (collision-induced dissociation mass spectrometry). For this purpose, the use of a chlorine containing HABI gives the opportunity to draw conclusions whether the photoproduct contains chlorine or not. NMR experiments were carried out to obtain a deeper insight into the thiol-thione equilibrium of heterocyclic RS-H. This equilibrium depends on the surrounding medium, and it strongly affects the reactivity of the **L-L**/RS-H system. This was studied by photo-DSC measurements upon exposure in the UV. Combination of these experiments extends the consideration into such photoinitiating systems.

2. Experimental Section

2.1 Materials

2,2'-Bis(2-chlorophenyl)-4,4',5,5'-tetraphenyl-1,1'-bi-1H imidazole, also known as *o*-Cl-HABI (**L-L**), was obtained as a scientific gift from Hampford Research. The thiols *4H*-1,2,4-triazole-3-thiol (**Ia**), 4-methyl-*4H*-1,2,4-triazole-3-thiol (**Ib**), 5-phenyl-*4H*-1,2,4-triazole-3-thiol (**Ic**), 5-*t*-butyl-*4H*-1,2,4-triazole-3-thiol (**Id**), 5-mercapto-1-phenyl-*1H*-tetrazol (**Ie**) were kindly donated by FEW Chemicals GmbH. The photolysis product 2,4,5-triphenylimidazol was available in the lab. Deuterated solvents were purchased from ARMAR. 2-Mercapto-1-methylimidazol (**If**), 1-docecanthiol (**II**), and the monomer 1,6-hexanediol diacrylate (HDDA) were purchased from Sigma-Aldrich. All other lab chemicals needed for the measurements were obtained from Sigma-Aldrich either.

2.2 Photolysis Experiments

A Hg–Xe 200 W UV lamp (LOT-Oriel) in combination with a water filter and a 320-380 nm broadband filter was used to generate lophyl radicals by irradiation of *o*-Cl-HABI dissolved in CD_3CN. The light entered a fiber connected with a temperature-controlled cuvette holder QPOD (Ocean Optics) equipped with a Peltier element and TC125 temperature controller (Ocean Optics). Exposure measurements were carried out in a 2 mm cuvette in which 1.8 mg *o*-Cl-HABI and 12 mg of the *4H*-1,2,4-triazole-3-thiol (**Ia**) were dissolved in 0.7 mL CD_3CN and exposed at 298K for 10 h. The solutions exposed were transferred to the LC-MS experiments.

2.3 Photo-DSC Experiments

A DSC Q-300 from TA instruments was synchronized with a Omnicure Series 2000-XLA with appropriate y-fiber optics, which equally directed the light on both sensors using the PCA-kit available from TA-instruments. Insertion of a broadband filter results in exposure at 320-380 nm using a mid-pressure mercury lamp while the main part of the emission originates from the 365 nm Hg emission line. An amount of 0.1 mol% *o*-Cl-HABI and 0.67 mol% of the corresponding co-initiator RSH was dissolved in HDDA at a temperature of 50 °C. The time required to dissolve the mercapto compounds depended on their structure (**Ia**: 1h; **Ib**: 2h; **Ic**:10h; **Id**: 3h; **Ie**: 4h; **If**: 2h; **II**: 1h). The samples were placed in an uncovered tzero aluminium pan with a weight of 5 mg under nitrogen purge of 50 mL min^{-1}. Equilibration of each sample was completed for 15 min prior to exposure. The samples were irradiated for a period of 5 minutes under constant exposure power of 25 $mW \times cm^{-2}$ at 25 °C. After irradiation, residual heat flow was monitored in a time frame of additional 10 minutes. The heat flow ($\dot{Q}$ in J/s) measured was divided by both the molar polymerization heat (ΔH_p) of HDDA (167 kJ/mol[50]) and the quantity of the monomer n_m (in mol) resulting in the polymerization rate (dx/dt in s^{-1}) as a function of time, Eq. 3.

$$\frac{dx}{dt} = \dot{x} = \frac{\dot{Q}}{\Delta H_p} \cdot \frac{1}{n_m} \quad (3)$$

In the next step, these data were numerically integrated with respect to the reaction time resulting in the fractional degree of polymerization x(t) as a function of time, Eq. 4. Some samples were poured into MeOH to determine the amount on insoluble crosslinked polymer.

$$x(\mathrm{t}) = \int_0 \dot{x}\, dt \quad (4)$$

2.4 NMR Study of tautomerism

A Bruker Fourier-300 MHz spectrometer was used for all NMR measurements. The mercapto compound was dissolved in HDDA at a concentration of 0.05 M. The resulting solution was transferred into the NMR-tube containing a capillary filled with $CDCl_3$ being necessary to obtain the *log*-signal. ^{1}H-NMR spectroscopy was applied to study the thiol-thione tautomer equilibrium in HDDA.

2.5 LC-MS analysis of photolysis products

Reaction products were analyzed by **u**ltra **p**erformance **l**iquid **c**hromatography coupled to **e**lectro**s**pray **i**onization **q**uadrupole **t**ime–**o**f–**f**light **m**ass **s**pectrometry (UPLC-ESI-QTOF-MS). On this account, diluted samples were injected onto an Acquinity UPLC system (Waters, Eschborn/Germany) mounted with a HSS T3 column and separated using a binary gradient. Eluting compounds were detected in positive and negative ionization mode from *m/z* 50 – 1000 using a MicroTOF–Q I hybrid quadrupole time-of-flight mass spectrometer equipped with an Apollo II electrospray ion source (Bruker Daltonics, Billerica, MA, USA). All mass spectra were acquired in centroid mode and recalibrated on the basis of lithium formiate cluster ions. Reaction products were extracted by visual inspection of base peak chromatograms (isolation width: ± 0.02 Da) and identified on the basis of their accurate mass and their collision-induced dissociation (CID) mass spectrum. For acquisition of CID mass spectra quasi-molecular cluster ions were isolated at the Q1 (isolation width: ± 3) and fragmented inside the collision cell using argon as collision gas. Product ions were detected as already described. More details can be found in the electronic supporting information.

P1 (3-[2-(4,5-diphenyl-1*H*-imidazol-2-yl)phenyl]-4,5-dihydro-1*H*-1,2,4-triazole-5-thione): ESI(+)-CID-MS/MS of m/z 396.13, $[M+H]^+$, CE = 40 eV; *m/z* (rel. int. (%)) = 327.0936 (100, $C_{21}H_{15}N_2S^+$), 293.1058 (17.4, $C_{21}H_{13}N_2^+$), 250.0534 (2.8, $C_{15}H_{10}N_2S^{\bullet+}$), 249.0469 (2.1, $C_{15}H_9N_2S^+$), 224.0507 (6.7, $C_{14}H_{10}NS^+$), 223.0437 (5.4, $C_{14}H_9NS^{\bullet+}$), 218.0823 (6.7, $C_{15}H_{10}N_2^{\bullet+}$), 217.0755 (2.5, $C_{15}H_9N_2^+$), 193.0876 (45.5, $C_{14}H_{11}N^{\bullet+}$), 167.0846 (28.7, $C_{13}H_{11}^+$), 165.0693 (11.3, $C_{13}H_9^+$), 152.0615 (6.1, $C_{12}H_8^{\bullet+}$).

P2 (2-(2-chlorophenyl)-4,5-diphenyl-1*H*-imidazole): ESI(+)-CID-MS/MS of m/z 331.1, $[M+H]^+$, CE = 40 eV; *m/z* (rel. int. (%)) = 331.0979 (2, $C_{21}H_{16}ClN_2^+$), 295.1217 (3.7, $C_{21}H_{15}N_2^+$), 194.0944 (49.2, $C_{14}H_{12}N^+$), 193.0874 (100, $C_{14}H_{11}N^{\bullet+}$), 177.0681 (8, $C_{14}H_9^+$), 176.0614 (4.5, $C_{14}H_8^{\bullet+}$), 167.0841 (84.7, $C_{13}H_{11}^+$), 165.0691 (79.3, $C_{13}H_9^+$), 152.0612 (68.1, $C_{12}H_8^{\bullet+}$), 125.014 (2.4, $C_7H_6Cl^+$), 117.0557 (12.1, $C_8H_7N^{\bullet+}$), 116.0483 (20.6, $C_8H_6N^+$).

P3 (2,4,5-triphenyl-1*H*-imidazole): ESI(+)-CID-MS/MS of m/z 297.14, $[M+H]^+$, CE = 40 eV; *m/z* (rel. int. (%)) = 297.1375 (1.5, $C_{21}H_{17}N_2^+$), 193.0877 (100, $C_{14}H_{11}N^{\bullet+}$), 192.0795 (10.3, $C_{14}H_{10}N^+$), 177.0684 (6.6, $C_{14}H_9^+$), 176.0609 (4.8, $C_{14}H_8^{\bullet+}$), 167.0837 (63.3, $C_{13}H_{11}^+$), 165.0688 (72.5, $C_{13}H_9^+$), 152.0611 (72.6, $C_{12}H_8^{\bullet+}$), 151.0531 (5.1, $C_{12}H_7^+$), 141.0685 (2.3, $C_{11}H_9^+$), 117.0554 (13.5, $C_8H_7N^{\bullet+}$), 116.0478 (20.7, $C_8H_6N^+$), 104.0473 (2.1, $C_7H_6N^+$).

P4 (2-(2-chlorophenyl)-4,5-diphenyl-imidazol-1-ylium): ESI(+)-CID-MS/MS of m/z 329.08, $[M+H]^+$, CE = 40 eV; *m/z* (rel. int. (%)) = 329.0822 (25.1, $C_{21}H_{14}ClN_2^+$), 294.1142 (6.1, $C_{21}H_{14}N_2^{\bullet+}$), 192.0784 (6.1, $C_{14}H_{10}N^+$), 165.071 (100, $C_{13}H_9^+$).

P5$_a$ (1-[2-(2-chlorophenyl)-4,5-diphenyl-2*H*-imidazol-2-yl]-2,4,5-triphenyl-1*H*-imidazol-3-ium): ESI(+)-CID-MS/MS of m/z 625.22, $[M+H]^+$, CE = 40 eV; *m/z* (rel. int. (%)) = 625.2125 (100, $C_{42}H_{30}ClN_4^+$), 488.2102 (3.7, $C_{35}H_{26}N_3^+$), 432.127 (4, $C_{28}H_{19}ClN_3^+$), 329.0817 (3.1, $C_{21}H_{14}ClN_2^+$), 194.0965 (10.4, $C_{14}H_{12}N^+$).

P5$_b$ (1-[2-(2-chlorophenyl)-4,5-diphenyl-2*H*-imidazol-2-yl]-2,4,5-triphenyl-1*H*-imidazol-3-ium): ESI(+)-CID-MS/MS of m/z 625.22, $[M+H]^+$, CE = 40 eV; *m/z* (rel. int. (%)) = 625.2145 (100, $C_{42}H_{30}ClN_4^+$), 488.2109 (63.1, $C_{35}H_{26}N_3^+$), 472.194 (3.5, $C_{35}H_{24}N_2^{\bullet+}$), 432.1344 (7.6, $C_{30}H_{16}N_4^{\bullet+}$), 419.1346 (4.4, $C_{28}H_{20}ClN_2^+$), 396.1543 (2.7, $C_{27}H_{23}ClN^+$), 385.1685 (39.2, $C_{28}H_{21}N_2^+$), 322.1392 (12.3, $C_{21}H_{21}ClN^+$), 306.118 (8, $C_{22}H_{14}N_2^{\bullet+}$), 295.1143 (7, $C_{20}H_{13}N_3^{\bullet+}$), 207.0897 (2, $C_{14}H_{11}N_2^+$), 194.0956 (17.8, $C_{14}H_{12}N^+$), 193.0876 (7.7, $C_{14}H_{11}N^{\bullet+}$), 180.0832 (29.7, $C_{13}H_{10}N^+$), 167.0864 (18.3, $C_{13}H_{11}^+$), 165.0694 (2.7, $C_{13}H_9^+$), 152.063 (4.4, $C_{12}H_8^{\bullet+}$).

L-L (1H-imidazole, 2-(2-chlorophenyl)-1-[2-(2-chlorophenyl)-4,5-diphenyl-2H-imidazol-2-yl]-4,5-diphenyl): ESI(+)-CID-MS/MS of m/z 659.18, $[M+H]^+$, CE = 40 eV; *m/z* (rel. int. (%)) = 329.082 (100, $C_{21}H_{14}ClN_2^+$), 294.1126 (4.5, $C_{21}H_{14}N_2^{\bullet+}$), 226.0405 (23.8, $C_{14}H_9ClN^+$), 192.0792 (11.5, $C_{14}H_{10}N^+$), 191.0713 (5.9, $C_{14}H_9N^{\bullet+}$), 165.0692 (28.2, $C_{13}H_9^+$), 122.998 (5.4, $C_7H_4Cl^+$).

Ia: ESI(-)-CID-MS/MS of m/z 100, $[M-H]^-$, CE = 10 eV; *m/z* (rel. int. (%)) = 99.997 (100, $C_2H_2N_3S^-$), 71.989 (2, $C_2H_2NS^-$).

2.6 Electrochemical Experiments

The electrochemical investigations were carried out with a three-electrode setup using platinum disks as working respectively auxiliary electrode and Ag/AgCl as reference electrode. For all measurements, Ferrocene was used as an internal standard and 0.1 M tetrabutylammonium hexafluorophosphate (Bu_4NPF_6) as supporting electrolyte. The half wave potentials of the internal standard Ferrocene usually amounted to 0.51 eV, which was checked prior to each series of measurements. The compounds studied were dissolved in absolute acetonitrile (water content ≤0.001%, from Sigma-Aldrich) with a concentration of 0.003 M. All solutions were purged with nitrogen prior to each measurement. Cyclic voltametry was performed with a Solartron 1285 Potentiostat at a scan rate of 15 mV s^{-1}. It started with measuring of an entire cycle of the respective compound. The measurements of the oxidation and reduction potentials of the compounds were carried out separately from each other. The measured cyclic voltamograms were evaluated using a self-developed software. The HOMO and LUMO energies were

calculated from the respective half wave potentials according to the eq. 5:

$$E^{HOMO/LUMO} = [-(E_{onset\ (vs.\ Ag/AgCl)} - E_{onset\ (Fc/Fc+\ vs.\ Ag/AgCl)})] - 4{,}8eV \quad (5)$$

In the cases where no oxidation or reduction peak was found, the HOMO and LUMO energies were calculated by the optical gap ΔE from the UV-Vis spectra using tangent method.

3. Results and Discussion

3.1 Selection of Materials

Excitation of **L-L** quantitatively results in formation of two lophyl radicals **L**· with a quantum yield of ≈2 with respect to **L**·[38]. The lophyl radical formed efficiently reacts with heterocyclic mercapto compounds **I**, which were selected from 5-membered heterocycles derived from triazole (**Ia-d**), tetrazole (**Ie**), and imidazole (**If**). The different materials compiled in the general structure **I** possess different redox potentials, and therefore, different HOMO-LUMO energies, electron density in the heterocycle, and bond dissociation energy of the S-H bond.

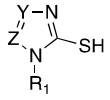

I

abbreviation	R_1	Y	Z
Ia	H	N	CH
Ib	CH_3	N	CH
Ic	H	N	C-Phenyl
Id	H	N	C-*t*-Butyl
Ie	Phenyl	N	N
If	CH_3	CH	CH

The general structure shown in **I** exhibits one possible tautomeric form; that is the thiol in this case. Principally, the thiol coexists in an equilibrium together with the tautomeric thione, Eq. 6. This equilibrium depends on the surrounding solvent. Thus, one needs to ask, which tautomeric form significantly affects the initiation of photopolymerization. The thiol should favor a mechanism based on hydrogen abstraction while the thione may result in a different. ^{1}H-NMR spectra exhibit the ratio of thiol/thione in the monomer used that is HDDA in our experiments.

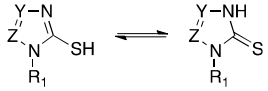

(6)

We also chose the aliphatic mercapto compound **II**, in which no thione exists. Thus, **II** represents a system for a hydrogen transfer mechanism with no alternatives.

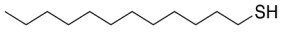

II

The HDDA monomer efficiently crosslinks. We chose a photo-DSC setup to study the efficiency of the photoinitiating system comprising **L-L** and the mercapto compound selected either from **I** or **II**.

3.2 Reactivity of the HABI-Mercapto Systems

Photo-DSC measurements easily provide information regarding the reactivity of photoinitiating systems containing crosslinking monomers. The maximum rate of polymerization $\mathbf{v_{max}}$ and the time being necessary to reach $\mathbf{v_{max}}$ empirically relate to the reactivity of the initiator system in the crosslinking material. The higher $\mathbf{v_{max}}$ the shorter must be $\mathbf{t_{max.}}$ A large $\mathbf{v_{max}}$ corresponds to a high reactive and efficient photoinitiating system. Figure 1 represents one possible example for photoinduced crosslinking of HDDA initiated by the initiator combination **L-L** and **Ia** showing the reactivity parameters $\mathbf{v_{max}}$ and $\mathbf{t_{max.}}$. The limiting conversion (x_∞) typically depends on available free volume, reaction temperature, and functionality of the monomer chosen.

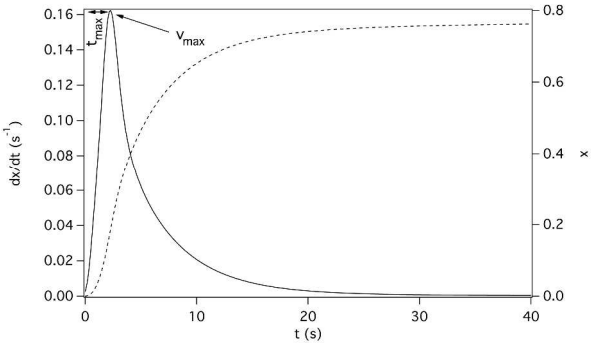

Figure 1: Photopolymerization of HDDA (99.4 wt%) initiated by the system **L-L** (0.1 mol%) and **Ia** (0.67 mol%) using the photo-DSC setup described

Table 1 shows the results obtained for photopolymerization of HDDA using different **L-L**/RSH systems. The aliphatic mercapto compound **II**, which cannot form any thione, exhibits the lowest reactivity in this series. The reactivity of **II** is close to a system without any mercapto compound. It has been well accepted, that HABIs without any coinitiator do not function as initiators in radical photopolymer systems[1-3].

Table 1: Determined maximum polymerization rates $\mathbf{v_{max}}$ and the time $\mathbf{t_{max}}$ to reach $\mathbf{v_{max}}$ during photopolymerization of HDDA using the initiator system consisting of *o*-Cl-HABI (0.1 mol%) and the investigated co-initiators **I** and **II** (0.67 mol%). As reference, photoinitiated polymerization was studied **without** any coinitiator.

Coinitiator	v_{max} (10^{-3} s^{-1})	t_{max} (s)
Ia	162	2.2
Ib	40	18.3
Ic	144	1.6
Id	72	7.8
Ie	182	1.4
If	5	88.9
II	2	284
without	1	1859

Data compiled in Table 1 allow to get a drawback regarding the reactivity of the HABI/RSH systems in HDDA. Thus, one can write the following series that generally splits into three groups:

Ie > **Ia** > **Ic** >> **Id** > **Ib** >> **If** > **II** > **without**.

The mercapto compounds **Ie**, **Ia**, and **Ic** exhibit the highest reactivity derived from heterocycles with distinct electron density

in the heterocyclic ring. Nevertheless, the alkyl substituted triazoles **Id** and **Ib** result in a reactivity that is significantly lower compared to **Ie**, **Ia**, and **Ic**. There is no clear correlation between the substitution pattern of the triazole moiety and photopolymerization reactivity measured. Moreover, the imidazole compound **If** exhibits the lowest reactivity in the series of the heterocyclic mercapto compounds although it possesses the lowest S-H bond dissociation energy (322 kJ/mol) compared to **Ia** and **Ie** showing both a S-H bond dissociation energy of 365 kJ/mol[32]. Nevertheless, the reactivity investigated in sensitized HABI/RSH systems[32] fairly shows a similar tendency in comparison with **Ie**, **Ia** and **If** in our directly photolysed HABI/RS-H systems. These results indicate that a discussion of reactivity cannot be exclusively explained by hydrogen abstraction mechanism[3]. Further reactions may compete with H-abstraction in the HABI/RSH system. This is supported by comparison with data of the aliphatic thiol **II** exhibiting the lowest efficiency of all coinitiators. Structure **II** allows only hydrogen abstraction by a precursor radical. The tautomeric equilibrium may provide alternative reaction routes.

Moreover, the reactivity of **L•** with RSH also strongly depends on the surroundings. Irradiation of **L-L** in HDDA showed a fast loss of **L•** absorbance after addition of **Ia** while **II** resulted in a slower reaction between **L•** and **II** (see supporting information for more details). However, a faster reactivity of **II** with **L•** was observed in DMSO showing that H-abstraction can also compete by change of the surrounding. This would be important for selection of the monomer. Nevertheless, analysis of the sample exposed in the photo-DSC setup showed an almost quantitative conversion of soluble HDDA into crosslinked polymer using **Ia** as coinitiator while **II** gives only 15% insoluble polymer under similar conditions (more details in supporting information). This demonstrates again the higher reactivity of **Ia** in comparison with **II** in HDDA.

3.3 Tautomerism of the Mercapto Compounds

NMR experiments focused to study the thiol-thione equilibrium existing in compounds of the general structure **I**. We chose two compounds with high and low reactivity; that is **Ia** and **If**, respectively. Both only differ in the Y-position of **I**.

Figure 2 shows the NMR-spectrum of **Ia** in HDDA. It exhibits typical protons assigned to the tautomeric thione-form. Integration of the overall ^{1}H-NMR spectrum yields the amount of each proton. In this experiment we found that 79% thione exists though this depends on the polarity of the solvent. Thus, the spectrum in d_6-DMSO results in almost quantitative formation of the thione form. Therefore, a more detailed understanding requires to take the NMR spectrum in the monomer chosen for radical polymerization. The insertion of $CDCl_3$ in fused capillaries in the NMR-tube allows to obtain the necessary *log*-signal.

Almost no thione was found in the case of **If** dissolved in HDDA (Figure 3) although it possesses a large amount of thione in d_6-DMSO (≈100%). The higher reactive **Ia** shows a higher contribution of thione in HDDA while the less reactive **If** does not exhibit any thione in the HDDA monomer measured by ^{1}H-NMR spectroscopy. **If** exhibits a reactivity comparable with the reference compound **II**, which cannot form any thione tautomer. Thus, it is obviously that a certain amount of thione significantly increases photopolymerization reactivity.

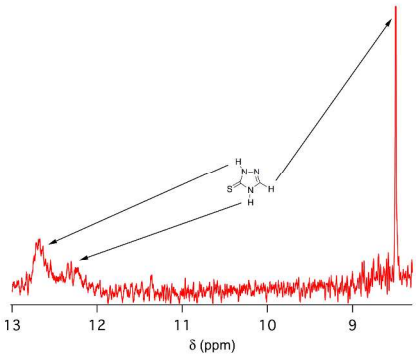

Figure 2: ^{1}H-NMR spectrum of **Ia** dissolved in HDDA

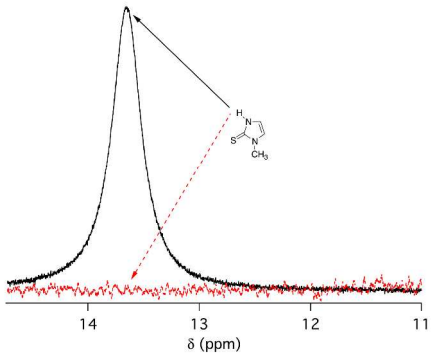

Figure 3: Signal of the proton bound at the nitrogen-atom of thione-tautomer of **If** in DMSO-d6 (red) and in HDDA (black) in the ^{1}H-NMR spectrum

On the other hand, no clear correlation exists between thione content in HDDA and photopolymerization reactivity (**Ia** > **Id** > **Ib**). ^{1}H-NMR measurements indicated high thione contents in alkyl substituted triazole derivatives (**Ia**: 64%; **Id**: 100%, **Ib**: 90%). Furthermore, determination of thione was not possible in the phenyl-substituted heterocycles **Ic** and **Ie** because H-exchange may occur between more available tautomers.

3.4 Photolysis Products

The reaction mixture obtained after exposure of **L-L** and **Ia** was investigated by UPLC-ESI-QTOF-MS to gain more information about the photolysis products formed. This analysis is necessary because the occurring mechanism appears to be more complicated as previously assumed[3]. Figure 4 shows a typical chromatogram of the reaction mixture. **L-L** (appearing at 900 s) nearly completely converted into photolysis products from which the main products **P1**-**P5** resulted.

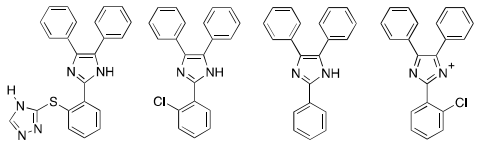

Ia only shows a mass spectrum after ionization in the negative mode (injection peak at 30 s). This signal clearly diminishes after reaction (data not shown).

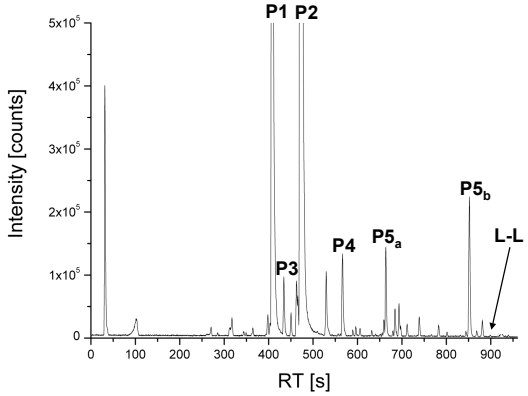

Figure 4: UPLC-ESI(+)-QTOF-MS base peak chromatogram (*m /z* 100 – 700) of an irradiated mixture comprising **Ia** and **L-L** (elemental composition: **P1**: $C_{23}H_{18}N_5S^+$, **P2**: $C_{21}H_{16}ClN_2^+$, **P3**: $C_{21}H_{17}N_2^+$, **P4**: $C_{21}H_{14}ClN_2^+$, **P5a**: $C_{42}H_{30}ClN_4^+$, **P5b**: $C_{42}H_{30}ClN_4^+$, **L-L**: $C_{42}H_{29}Cl_2N_4^+$, more details in electronic supporting information).

Interestingly, the photolysis products **P1** and **P3** do not contain any chlorine because the MS does not exhibit the expected isotope ratio (more details in electronic supporting information). Thus, chlorine must be released somehow during photolysis. The identity of **P3** was confirmed by measuring the in-house available reference substance. As a proposal, photolysis product **P1** can be explained as an addition product of **L**· and **Ia**, because the CID-MS shows a loss of a triazole unit ($C_2H_3N_3$) resulting in a fragment at 327.09 amu. This exhibits the elemental composition $C_{21}H_{15}N_2S^+$ and bears a sulfur at the triphenylimidazol skeleton. Furthermore, **P1** exhibits a similar CID-MS compared to **P3**. These are the fragments found at 193.09, 167.08, 165.07 and 152.06 amu confirming the identity of a triphenylimidazole skeleton.

Furthermore, chlorine-containing **P2** was assigned as further photolysis product. It exhibits the typical isotope ratio of a chlorine containing material (more details in electronic supporting information). **P4** was identified as a cation. The fragments found in the CID-MS indicate the presence of a triphenylimidazole skeleton either. Products **P5a** and **P5b** were most likely formed by cross coupling of a chlorine-bearing and chlorine-free triphenylimidazolyl radical. Both are isomers with the same mass (compare caption of Figure 4).

3.5 Mechanistic Aspects

Based on literature[29, 51], one could propose a mechanism describing electron transfer of RS-H into the hole of photoexcited HABI (**L-L***) explaining formation of the lophine **P2**, eq. 7. Such mechanistic discussions of *o*-Cl-HABI were previously described in **L-L**/leuco dye systems [1, 2].

$$L-L^{*}+RS-H \rightarrow L-L^{-\bullet}+RS-H^{+\bullet} \quad (7)$$

This would thermodynamically be possible resulting in oxidation of the heterocyclic mercapto compound ($RS\text{-}H^{+\cdot}$) and formation of the reduced HABI ($\mathbf{L_2}^{-\cdot}$). $RS\text{-}H^{+\cdot}$ could form a thiyl radical by release of a proton. The redox potentials measured for *o*-Cl-HABI and the mercapto compounds would support such a proposal only for some of the heterocyclic compounds **I**, Table 2. **L-L** possesses an oxidation potential of 1.58 V corresponding to a HOMO energy of -5.81 eV. According to the data of **I** compiled in Table 2, all thiols/thiones except for **Ie** should follow this proposal, because their HOMO energies locate higher compared to **L-L**. On the other hand, **Ie** exhibited the best photoinitiation reactivity but had the lowest oxidation capability. Furthermore, the imidazole derivative **If** showed a low initiation efficiency but the best oxidation capability. If electron transfer would dominate according to eq. 7, one should observe a clear correlation between the free energy of electron transfer and photoinitiation efficiency. This is not really supported by our data. In addition, a mechanism in which **L**· would be reduced by the mercapto compound can be excluded either due to its reduction potential; that is E_{red} (**L**·/**L**$^-$) = -0.15 V (measured against the ferrocene/ferrocenium potential)[52].

Table 2: Oxidation potentials (E_{ox}) and respective HOMO energies of **I** measured in acetonitrile. ΔE represents the energy difference between the HOMO of **L-L** and the HOMO of **I**

Compound	E_{ox} (V)	HOMO (eV)	ΔE (eV)[a)]	Reactivity scale
Ie	1.89	-5.99	0.18	1
Ic	1.54	-5.65	-0.16	3
Id	1.43	-5.37	-0.44	4
Ib	1.06	-5.23	-0.58	5
Ia	0.94	-5.06	-0.75	2
If	0.83	-4.98	-0.83	6

[a)] $\Delta E = (HOMO_{L\text{-}L}\text{-}HOMO_{RS\text{-}H})$

The formation of chlorine free photoproducts **P1** and **P3** as well as mixed photoproducts **P5a** and **P5b** shows that alternative reactions presumably explain formation of thiyl radicals in our system. Therefore, a mechanistic discussion should more or less focus on the electron density distribution comparing **Ia** and **If**. According to its electronic property, **L**· belongs to a nucleophilic radical[53]. Most of its unpaired electron density locates in the *p*-orbitals of the SOMO (compare Figure S1 in ESI). In addition, nucleophilic radicals possess a low capability to abstract hydrogen from appropriate donors, which are for example aliphatic thiols. This would require unpaired electron density in the *s*-orbitals of the SOMO because H-abstraction results in formation of a σ-bond. Our experiments showed a low reactivity of **L**· with **II**, that experimentally proves the nucleophilic property of **L**·. Thus, H-abstraction should occur with lower efficiency as experimentally shown by data in Table 1.

Nucleophilic radicals prefer to interact with the LUMO of a conjugated system; that is in our case the reaction of **L**• with the heterocycle **I**. The larger the atomic orbital coefficients in the LUMO the larger the interaction energy, and thus, the reactivity according to the perturbation theory[53]. This refers for example to the C-atoms in 4 and 5 position of **If** and 5-position of **Ia** (compare the patterns in electronic supporting information). MO-calculations of **If** showed for the LUMO nearly no electron density at the 4 and 5 position if this exists as thiol. Thus, the low reactivity of **If** is therefore a result of the low interaction between **L**• and **If**, which exists in HDDA only as thiol. This agrees with our experimental findings where **L**• exhibits low reactivity with **II**. On the other hand, remarkable electron density exists for the C-atoms at the 5-position of **Ia** considering the thione tautomer. This must lead to a better interaction of the heterocycle **Ia** with

L• resulting in an increased reactivity. HDDA favors formation of the thione tautomer of **Ia** as shown by NMR.

An addition elimination mechanism as shown in Figure 5 would explain formation of chlorine free photoproducts, i.e. **P1** and **P3** as well as the mixed photoproducts **P5a** and **P5b**, and formation of initiating radicals In•. Both, **P1** and **P2** are major products. Formation of **P2** can alternatively occur according to H-abstraction[1,2,38]. The release of highly reactive chlorine concluded from MS analysis of photoproducts may explain the high reactivity of *o*-Cl-HABI, which can compete with photoinitiators grouped in the IRGACURE series.

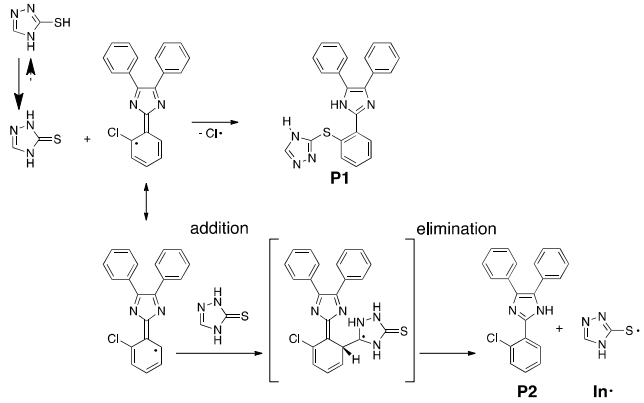

Figure 5: Proposal for the extended mechanistic formation of initiator radicals (Cl· and **In**·) during exposure of **L-L** in the presence of the thione of **Ia**.

4. Conclusions

Results obtained would require to extend the mechanism regarding the formation of initiator radicals in the case of a photoinitiator system comprising **L-L** and a heterocyclic mercapto compound. Mercapto compounds, which are able to form the tautomeric thione, exhibit a higher reactivity. This tautomeric form reacts fast with the lophyl radical resulting in generation of initiating thiyl radicals although competitive reactions such as H-abstraction or electron transfer according to eq. 7 may occur with lower efficiency leading to the same initiating species – the thiyl radical. The surrounding matrix influences these competing reactions. Furthermore, the relatively low sensitivity of the lophyl radical against oxygen may be a further benefit of this system explaining the high photoinitiating reactivity.

Further research of systems comprising **L-L** should focus on multifunctional heterocyclic thiol/thione compounds keeping in mind that the thione responsibly affects photoinitiation efficiency in acrylic monomers. Such multifunctional heterocycles could be easily built up by the reaction of a multifunctional amine and thiosemicarbazide. This may lead to higher crosslinking densities of the crosslinked acrylate because formation of the initiating thiyl radical occurs at a higher functional moiety. Triazoles based on structure **Ic** depict a reasonable basis of such an approach because even this structure showed a high reactivity in HDDA while alkyl substituted compounds based on **Id** would result in a decrease of initiation efficiency.

Solubility of *o*-Cl HABI in common coatings can be seen as one issue to make this system more attractive for a broader range of applications. This can be achieved by incorporation of substituents improving the solubility. Nevertheless, these changes should not influence the reactivity of HABI in combination with thiol/thione compounds.

Further mechanistic studies should also clarify the function of chlorine in the HABI skeleton. Perhaps, a modification with more halogens at the ring would bring new impetus in this field since the release of chlorine as reactive and additional initiating species has been discussed as a matter of fact in this contribution. Thus, we believe that further mechanistic studies will bring new progress to develop efficient photoinitiating systems. This requires a extended mechanistic concept.

[a] *Department of Chemistry and Institute for Coatings and Surface Chemistry, Niederrhein University of Applied Sciences, Adlerstr. 32, D-47798 Krefeld, Germany. Fax: +49 2151 8224195; Tel: +49 2151 822 4075; E-mail: bernd.strehmel@hsnr.de, veronika.strehmel@hsnr.de*
[b] *Leibniz Institute of Plant Biochemistry, Weinberg 3, D-06120 Halle, Germany.*
[c] *Thuringian Institute of Textile and Plastics Research e.V, Breitscheidstraße 97, D-07407 Rudolstadt, Germany.*

Acknowledgment

VS gratefully acknowledges the Federal Ministry of Education and Research for financial support within the "Professorinnenprogramm" (grant# 01FP09231 C).

Notes and references

1. R. Dessauer, *Photochemistry, History and Commercial Applications of Hexaarylbiimidazoles: All about HABIs*, Elsevier, 2006.
2. R. Dessauer, The invention of Dylux instant-access imaging materials and the development of HABI chemistry - a personal history, *Adv. Photochem.*, 2005, **28**, 129-261.
3. B. M. Monroe and G. C. Weed, Photoinitiators for free-radical-initiated photoimaging systems, *Chem. Rev.*, 1993, **93**, 435-448.
4. V. Strehmel, J. V. Whishart, D. A. Polyansky and B. Strehmel, Recombination of Photogenerated Lophyl Radicals in Imidazolium-Based Ionic Liquids, *ChemPhysChem*, 2009, **10**, 3112 – 3118.
5. S. Berdzinski, J. Horst, P. Strassburg and V. Strehmel, Recombination of Lophyl Radicals in Pyrrolidinium-Based Ionic Liquids, *ChemPhysChem*, 2013, **24**, 1751-1760.
6. V. Strehmel, Radicals in ionic liquids, *ChemPhysChem*, 2012, **13**, 1649-1663.
7. K. Mutoh, M. Sliwa and J. Abe, Rapid Fluorescence Switching by Using a Fast Photochromic [2.2]Paracyclophane-Bridged Imidazole Dimer, *J. Phys. Chem. C*, 2013, **117**, 4808-4814.
8. S. Hatano, T. Horino, A. Tokita, T. Oshima and J. Abe, Unusual Negative Photochromism via a Short-Lived Imidazolyl Radical of 1,1'-Binaphthyl-Bridged Imidazole Dimer, *J. Am. Chem. Soc.*, 2013, **135**, 3164-3172.
9. K. Fujita, S. Hatano, D. Kato and J. Abe, Photochromism of a radical diffusion-inhibited hexaarylbiimidazole derivative with intense coloration and fast decoloration performance, *Org. Lett.*, 2008, **10**, 3105-3108.
10. K. Mutoh, E. Nakano and J. Abe, Spectroelectrochemistry of a Photochromic [2.2]Paracyclophane-Bridged Imidazole Dimer: Clarification of the Electrochemical Behavior of HABI, *J. Phys. Chem. A*, 2012, **116**, 6792-6797.
11. A. Kikuchi, T. Iyoda and J. Abe, Electronic structure of light-induced lophyl radical derived from a novel hexaarylbiimidazole with pi-conjugated chromophore, *Chem. Comm.*, 2002, 1484-1485.
12. H. Sato, K. Kasatani and S. Murakami, Magnetic field effects on the photochromism of hexaphenylbiimidazolyl, *Chem. Phys. Lett.*, 1988, **151**, 97-101.
13. Y. Sakaino, Structures and chromotropic properties of imidazole derivatives produced from 3,6-bis(4,5-diphenyl-2H-imidazol-2-ylidene)cyclohexa-1,4-diene, *J. Chem. Soc., Perkin Trans. 1*, 1983, 1063-1066.

14. Y. Sakaino, H. Kakisawa and T. Kusumi, Synthesis of new photochromic compounds from the dimer of arylphenanthroimidazoles, *J. Heterocyclic Chem.*, 1975, **12**, 953-956.
15. K. Maeda and T. Hayashi, Mechanism of photochromism, thermochromism, and piezochromism of dimers of triarylimidazolyl, *Bull. Chem. Soc. Jpn.*, 1970, **43**, 429-438.
16. T. Shida, K. Maeda and T. Hayashi, Optical and E.S.R. studies on triphenylimidazolyl radicals produced by photolysis and radiolysis at low temperatures, *Bull. Chem. Soc. Jpn.*, 1969, **42**, 3044.
17. M. A. J. Wilks and M. R. Willis, Kinetics of the photochromic decay reaction of 2,2',4,4',5,5'-hexaphenylbiimidazolyl, *J. Chem. Soc. B*, 1968, 1526-1529.
18. T. Hayashi, K. Maeda and T. Kanaji, The mechanism of the photochromism and thermochromism of 2,2',4,4',5,5'-hexaphenyl-1,1'-biimidazolyl in a solid state, *Bull. Chem. Soc. Jpn.*, 1965, **38**, 857.
19. J. V. Caspar, I. V. Khudyakov, N. J. Turro and G. C. Weed, ESR Study of Lophyl Free Radicals in Dry Films, *Macromolecules*, 1995, **28**, 636-641.
20. X. Z. Qin, A. Liu, A. D. Trifunac and V. V. Krongauz, Photodissociation of hexaarylbiimidazole. 1. Triplet-state formation, *J. Phys. Chem.*, 1991, **95**, 5822-5826.
21. A. D. Liu, A. D. Trifunac and V. V. Krongauz, Photodissociation of hexaarylbiimidazole. 2. Direct and sensitized dissociation, *J. Phys. Chem.*, 1992, **96**, 207-211.
22. T. Matsuura, Y. Ito and I. Saito, Photoinduced reactions. LXVIII. Photochemical dehydrogenation of imidazolines to imidazoles, *Bull. Chem. Soc. Jpn.*, 1973, **46**, 3805-3809.
23. T. Hayashi and K. Maeda, Mechanism of reversible photochemical color change of bis(triphenylimidazolyl) at low temperature, *Bull. Chem. Soc. Jpn.*, 1967, **40**, 2990.
24. J. Abe, T. Sano, M. Kawano, Y. Ohashi, M. M. Matsushita and T. Iyoda, EPR and density functional studies of light-induced radical pairs in a single crystal of a hexaarylbiimidazolyl derivative, *Angew. Chem., Internat. Ed.*, 2001, **40**, 580-582.
25. M. Schrödner, H. Schache, H. Lindauer, R. Schrödner and A. Konkin, Oscillations of the lophyl radical concentration during the photo-decomposition of o-Cl-hexaarylbisimidazole, *J. Photochem. Photobiol., A: Chem.*, 2012, **233**, 60-64.
26. A. Ibrahim, C. Ley, X. Allonas, O. I. Tarzi, A. Chan Yong, C. Carre and R. Chevallier, Optimization of a photopolymerizable material based on a photocyclic initiating system using holographic recording, *Photochem. Photobiol. Sci.*, 2012, **11**, 1682-1690.
27. X. Hu, H. Zhang, G. Zhang, Y. Sheng, Y. Wang and R. Zhao, Water-resisting compound red-sensitive photopolymer: mechanism and optimization of components, *Proc. SPIE*, 2005, **5636**, 635-645.
28. C. Zhang, J. Zhao, J. He, L. Li and Y. Yang, Photoinitiating systems and photopolymer materials for holography, *Proc. SPIE*, 1998, **3559**, 81-87.
29. D. F. Eaton, A. G. Horgan and J. P. Horgan, Mechanism of coinitiation of photopolymerization of methyl methacrylate by hexaarylbiimidazole-hydrogen atom donor combinations. The role of electron transfer versus direct hydrogen atom abstraction, *J. Photochem. Photobiol., A: Chem.*, 1991, **58**, 373-391.
30. X. Li, Y. Zhao, J. Wu, M. Shi and F. Wu, Two-photon photopolymerization using novel asymmetric ketocoumarin derivatives, *J. Photochem. Photobiol., A*, 2007, **190**, 22-28.
31. J. Xue, Y. Zhao, J. Wu and F. Wu, Novel benzylidene cyclopentanone dyes for two-photon photopolymerization, *J. Photochem. Photobiol., A*, 2008, **195**, 261-266.
32. J. Lalevee, F. Morlet-Savary, R. M. El, X. Allonas and J. P. Fouassier, Thiyl radical generation in thiol or disulfide containing photosensitive systems, *Macromol. Chem. Phys.*, 2009, **210**, 311-319.
33. S. Suzuki, P. Emilie, T. Urano, S. Takahara and T. Yamaoka, Three-component photoradical initiating system-the effect of 2-mercaptobenzothiazole as a coinitiator in polymer matrix, *Polymer*, 2005, **46**, 2238-2243.
34. S. Suzuki, T. Urano, K. Ito, T. Murayama, I. Hotta, S. Takahara and T. Yamaoka, Pyrromethene dye sensitized photopolymer and the application to visible laser direct imaging, *Journal of Photopolymer Science and Technology*, 2004, **17**, 125-130.
35. S. Suzuki, T. Urano, N. Miyagawa, S. Takahara and T. Yamaoka, Three-component radical photoinitiating systems - the effect of the accelerator, *Journal of Photopolymer Science and Technology*, 2001, **14**, 259-262.
36. T. Urano, H. Ito, K. Takahama and T. Yamaoka, Photopolymerization mechanisms of acrylates in poly(methyl methacrylate) films, *Polym. Adv. Technol.*, 1999, **10**, 201-205.
37. T. Urano, H. Ito, K. Takahama and T. Yamaoka, Double-amplified photoinitiator systems, *RadTech'98 North America UV/EB Conference Proceedings, Chicago, Apr. 19-22, 1998*, 1998, 734-745.
38. Q. Q. Zhu, M. Fink, F. Seitz, S. Schneider and W. Schnabel, On the photolysis of bis[2-(o-chlorophenyl)-4,5-diphenylimidazole] sensitized by 2-isopropylthioxanthone or Michler's ketone, *J. Photochem. Photobiol. A: Chem.*, 1991, **59**, 255-263.
39. M. Jin, J.-P. Malval, D.-L. Versace, F. Morlet-Savary, H. Chaumeil, A. Defoin, X. Allonas and J.-P. Fouassier, Two-photon absorption and polymerization ability of intramolecular energy transfer based photoinitiating systems, *Chem. Commun.*, 2008, 6540-6542.
40. X. Allonas, J. P. Fouassier, M. Kaji and Y. Murakami, Excited state processes in a four-component photosensitive system based on a bisimidazole derivative, *Photochem. Photobiol. Sci.*, 2003, **2**, 224-229.
41. X. Allonas, J. P. Fouassier, M. Kaji, M. Miyasaka and T. Hidaka, Two and three component photoinitiating systems based on coumarin derivatives, *Polymer*, 2001, **42**, 7627-7634.
42. X. Allonas, J. P. Fouassier, M. Kaji and M. Miyasaka, On the ability of coumarin derivatives to interact with photoinitiators, *Journal of Photopolymer Science and Technology*, 2000, **13**, 237-242.
43. T. Urano, Sensitizer dyes and sensitization mechanisms in photopolymer coating layer, *Proc. SPIE*, 2002, **4659**, 420-427.
44. T. Urano, M. Ishikawa, Y. Sato and H. Itoh, Sensitizer dyes and sensitization mechanisms in photopolymer coating layer II, *J. Photopoly. Sci. Technol.*, 1999, **12**, 711-716.
45. T. Urano, E. Hino, H. Ito, M. Shimizu and T. Yamaoka, Study of radical generated from coumarin dye-sensitized photoinitiator systems in high-speed photopolymer coating layers using laser flash photolysis, *Polym. Adv. Technol.*, 1998, **9**, 825-830.
46. T. Urano, H. Nagasaka, S. Shimizu, H. Ito, M. Shimizu, S. Takahara and T. Yamaoka, Laser-flash photolysis in high-speed photopolymer coating layers containing carbonylbiscoumarin dyes and 2,2'-bis(2-chlorophenyl)-4,4',5,5'-tetraphenyl-1,1'-bi-1H-imidazole, *Bull. Chem. Soc. Jpn.*, 1997, **70**, 1659-1664.
47. T. Urano, H. Nagasaka, M. Shimizu, S. Takahara and T. Yamaoka, Laser flash photolysis in high-speed photopolymer coating layers: effects of incorporating dimethyl phthalate as a plasticizer into coating formulation, *Bull. Chem. Soc. Jpn.*, 1996, **69**, 693-700.
48. T. Urano, H. Nagasaka, M. Tsuchiyama, S. Shimizu, K. Kawazoe, M. Shimizu and T. Yamaoka, Laser flash photolysis in high-speed photopolymer coating layers, *Bull. Chem. Soc. Jpn.*, 1995, **68**, 1661-1668.
49. W. A. Green, *Industrial Photoinitiators: A Technical Guide*, CRC Press, Boca Raton, 2010.
50. H.-J. Timpe and B. Strehmel, Lichtinduzierte Polymer- und Polymerisationsreaktionen. 44. Zur Kinetik der radikalischen Photopolymerisation mehrfunktionellerAcrylate in polymeren Bindemitteln, *Makromol. Chem.*, 1991, **192**, 779-791.
51. M. Muneer, P. V. Kamat and M. V. George, Electron transfer reactions. Reaction of nitrogen heterocycles with potassium, *Canadian Journal of Chemistry*, 1990, **68**, 969-975.
52. E. W. Oliver, D. H. Evans and J. V. Caspar, Electrochemical studies of a hexaarylbiimidazole, *J. Electroanal. Chem.*, 1996, **403**, 153-158.
53. I. Fleming and J. Podlech, *Molekülorbitale und Reaktionen organischer Verbindungen*, Wiley-VCH, Weinheim, 2012.

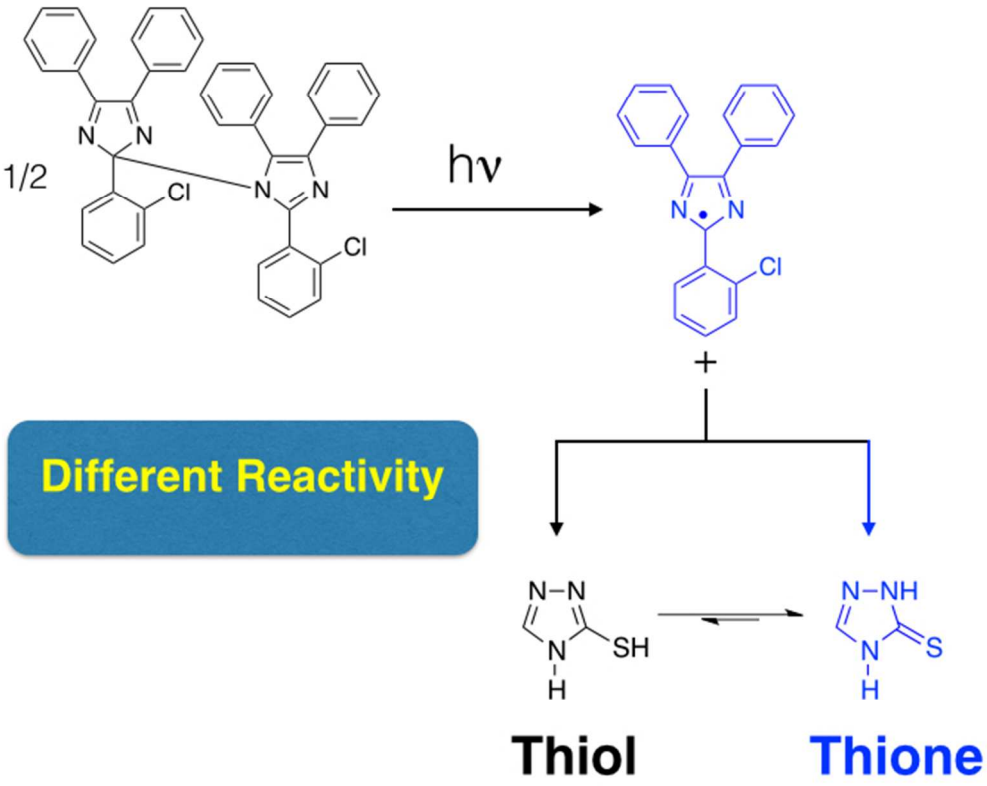

238x191mm (72 x 72 DPI)